

A peptomimetic inhibitor of BCL6 with potent antilymphoma effects in vitro and in vivo

Leandro C. Cerchietti,¹ Shao Ning Yang,¹ Rita Shaknovich,² Katerina Hatzi,¹ Jose M. Polo,³ Amy Chadburn,² Steven F. Dowdy,⁴ and Ari Melnick¹

¹Division of Hematology and Medical Oncology, Department of Medicine, and ²Department of Pathology, Weill Cornell College of Medicine, New York, NY;

³Developmental and Molecular Biology, Albert Einstein College of Medicine, Bronx, NY; and ⁴Howard Hughes Medical Institute and Department of Cellular and Molecular Medicine, University of California at San Diego School of Medicine, La Jolla

The BCL6 transcriptional repressor is the most commonly involved oncogene in diffuse large B-cell lymphomas (DLBCLs). BCL6 lymphomagenic activity is dependent on its ability to recruit corepressor proteins to a unique binding site on its N-terminal BTB domain. A recombinant peptide fragment of the SMRT (silencing mediator for retinoid and thyroid hormone receptor) corepressor that blocks this site can inhibit BCL6 biologic func-

tions. Shortening and conversion of this peptide to D-amino acid and retro configuration as well as the addition of a fusogenic motif yielded a far more potent and stable BCL6 inhibitor that still retained the specificity of the original SMRT fragment. Like the L-peptide, retroinverso BCL6 peptide inhibitor (RI-BPI) selectively killed BCR rather than OxPhos-type DLBCL cells. The RI-BPI could recapitulate the failure to form germinal centers

seen in BCL6 null mice yet was nontoxic and nonimmunogenic even when administered for up to 52 weeks. RI-BPI showed superior duration of tissue penetration and could accordingly powerfully suppress the growth of human DLBCLs xenografts in a dose-dependent manner. Finally, RI-BPI could kill primary human DLBCL cells but had no effect on normal lymphoid tissue or other tumors. (Blood. 2009;113:3397-3405)

Introduction

Expression of the B-cell lymphoma 6 (BCL6) transcriptional repressor is required for B cells to form germinal centers (GCs) and undergo immunoglobulin affinity maturation.^{1,2} BCL6 contributes to the GC B-cell phenotype of clonal expansion and genetic recombination by repressing target genes involved in DNA damage responses, such as *ATR*, *TP53*, and *CDKN1A*.³⁻⁵ BCL6 can also repress the *PRDM1* gene and thus inhibit plasma cell differentiation of GC B cells.^{6,7} Translocations or mutations of negative regulatory elements that occur as byproducts of class switch recombination or somatic hypermutation can lead to constitutive expression of BCL6.^{8,9} Such events are among the most common genetic lesions found in human diffuse large B-cell lymphoma (DLBCL).

BCL6 is a member of the BTB-POZ family of proteins. Homodimerization of the BCL6 BTB domain forms an extended lateral groove motif along the dimer interface, which is required to recruit the SMRT (silencing mediator for retinoid and thyroid hormone receptor) and N-CoR corepressors.¹⁰ Amino acid side chains protruding into this groove make extensive contact with an 18-residue BCL6-binding domain (BBD) peptide that is conserved between N-CoR and SMRT.¹⁰ The BCL6 lateral groove residues that contact N-CoR and SMRT are unique to BCL6 and are not present in other BTB proteins.¹⁰ A recombinant peptide containing the SMRT BBD along with a cell-penetrating TAT domain and other motifs was able to block interaction of BCL6 with SMRT and N-CoR. This BCL6 peptide inhibitor (BPI) could reactivate BCL6 target genes and kill BCL6-expressing DLBCL cell lines in vitro.¹¹ DLBCL cells thus require the continued presence and function of

BCL6 for their survival, suggesting that BCL6 is a bona fide therapeutic target in this disease.

Oncogenic transcription factors, such as BCL6, are ideal targets for the development of therapeutic inhibitors because they exert a profound influence on cellular phenotype. Directly targeting such factors could transcriptionally reprogram tumor cells to either revert to a normal phenotype or escape from aberrant survival programs. One of the main barriers thus far to development of such inhibitors is that most transcription factors mediate their effects through protein-protein interactions, which are often quite complex and may not be suited to inhibition by small molecules. In recent years, this limitation has been overcome by harnessing protein transduction domains (PTDs), such as the 9 residue cationic HIV-TAT motif.¹² PTDs allow even full-length proteins to be effectively transduced into virtually all cell types both in vitro and in vivo. The TAT PTD penetrates cells via macropinocytosis and enters the cytoplasm by leaking through the macropinosome membrane as the pH drops within.¹³ Coadministration of a fusogenic peptide from the influenza virus hemagglutinin protein can greatly facilitate escape of PTDs from macropinosomes.¹³ Because TAT also functions as a nuclear localization signal, it is well suited for the delivery of transcription factor inhibitors.

Based on this initial work, we hypothesized that BCL6 could be exploited as a therapeutic target in DLBCL. We report herein the development of a series of synthetic peptide inhibitors of BCL6, culminating in the generation of a retroinverso/fusogenic peptidomimetic molecule with superior potency and stability. This retroinverso

Submitted July 14, 2008; accepted September 25, 2008. Prepublished online as *Blood* First Edition paper, October 16, 2008; DOI 10.1182/blood-2008-07-168773.

An Inside *Blood* analysis of this article appears at the front of this issue.

The online version of this article contains a data supplement.

The publication costs of this article were defrayed in part by page charge payment. Therefore, and solely to indicate this fact, this article is hereby marked "advertisement" in accordance with 18 USC section 1734.

© 2009 by The American Society of Hematology

BPI (RI-BPI) inhibitor retained its specificity for BCL6 and could disrupt BCL6 repression complexes in DLBCL cells. RI-BPI was nontoxic and nonimmunogenic in animals, even when administered for up to 1 year. The peptide was also active against primary human DLBCL cells. RI-BPI is thus a promising BCL6-targeted therapy agent for translation to clinical trials in humans with DLBCL.

Methods

Cell lines

The DLBCL cell lines OCI-Ly1, OCI-Ly4, OCI-Ly7, and OCI-Ly10 (herein Ly1, Ly4, Ly7, and Ly10, respectively) were grown in medium containing 90% Iscove and 10% fetal calf serum (FCS), and supplemented with antibiotics, and the DLBCL cell lines Pfeiffer, Toledo, Farage, OCI-Ly3 (herein Ly3), SU-DHL6, and SU-DHL4 were grown in medium containing 90% RPMI and 10% FCS supplemented with antibiotics, L-glutamine, and *N*-2-hydroxyethylpiperazine-*N'*-2-ethanesulfonic acid. Cells were maintained in these conditions during the experiments, and peptides were added from a 1000× concentrated stock solution to the 10% serum-containing culture medium.

Primary cell treatment

Patient deidentified tissues were obtained in accordance with the guidelines and approval of the Institutional Review Board of the Albert Einstein College of Medicine. We obtained single-cell suspensions from lymph node biopsies by physical disruption of tissues (using scalpels and cell restrainers), followed by cell density gradient separation (Fico/Lite LymphoH; Atlanta Biologicals, Norcross, GA). Cell number and viability were determined by trypan blue dye exclusion, and cells were cultivated in medium containing 80% RPMI and 20% FCS supplemented with antibiotics, L-glutamine, and *N*-2-hydroxyethylpiperazine-*N'*-2-ethanesulfonic acid for 48 hours. Three different cell concentrations in triplicates were exposed to 3 doses of control and active peptides (1, 5, and 10 μM). After 48 hours of exposure, viability was determined using a fluorometric resazurin reduction method (CellTiter-Blue; Promega, Madison, WI) and trypan blue dye exclusion. The BCL6 protein status was determined in paraffin-embedded samples by immunohistochemistry using anti-BCL6 (Dako North America, Carpinteria, CA).

Mice xenotransplant models

All procedures involving animals followed National Institutes of Health protocols and were approved by and done according to guidelines of the Animal Institute Committee of the Albert Einstein College of Medicine (Bronx, NY). Six- to 8-week-old male SCID mice were purchased from the National Cancer Institute (Bethesda, MD) and housed in a barrier environment. Mice were subcutaneously injected in the left flank with low-passage 10⁷ human DLBCL cells (SU-DHL6, SU-DHL4, and Toledo). Tumor volume was monitored every other day using electronic digital calipers (Fisher Scientific, Pittsburgh, PA) in 2 dimensions. Tumor volume was calculated using the formula: tumor volume (mm³) = (smallest diameter² × largest diameter)/2. When tumors reached a palpable size (~75-100 mm³ after 19-36 days after injection depending on the cell line), the mice were randomly assigned to different treatment arms; in consequence, these experiments were all performed once tumors had fully formed in the animals. Peptides were administered by intraperitoneal injection. Mice were weighed every other day. All mice were killed by cervical dislocation under anesthesia when at least 2 of 10 tumors reached 20 mm in any dimension (equivalent to 1-g tumors) that for the cell lines used corresponded to day 10 (or 9 days of treatment). At the moment of death, blood was collected (StatSampler; Iris, Westwood, MA) and tumors and other tissues were harvested and weighted.

Peptides sequences, reporter assays, in vitro BPI binding, chromatin immunoprecipitation analysis, real-time PCR, growth inhibition determination, mice toxicity studies, mice GC models, human β2-microglobulin

determination, apoptotic index, proliferation index, mitotic index, BPI distribution in tumors, serum kinetics of BPI, immunogenicity studies, and statistics are provided in Document S1 (available on the *Blood* website; see the Supplemental Materials link at the top of the online article).

Results

Synthetic short forms of BPI preserve its antilymphoma activity

We previously reported that a recombinant BPI containing the SMRT 21-residue BBD could specifically inhibit the transcriptional repressor activity of the BCL6 BTB domain.¹¹ BPI consisted of 120 amino acids and also included a TAT domain for cellular penetration, an hemagglutinin (HA) tag for immunodetection, a (HIS)₆ tag for purification purposes, and linker sequences. Although BPI could kill DLBCL cells at low micromolar concentrations, it was highly unstable and required frequent readministration to cell cultures to detect its biologic activities.¹¹ Based on these proof-of-principle data, we hypothesized that inhibition of the BCL6 BTB domain might be an effective means for delivering targeted therapy against DLBCL. To test whether such an approach was feasible, we used a rational design strategy to generate superior inhibitors with drug-like properties that could be rigorously tested in vitro and in vivo and potentially translated to the clinic.

We chose DLBCL cell growth inhibition as the most relevant screening assay to compare and contrast the biologic activity of BPI and its derivatives. Recombinant BPI displayed an average growth inhibitory concentration 50% (GI₅₀) of 11.3 μM when given every 4 hours for a period of 48 hours (ie, dose frequency = 12) in dose-response experiments performed in 3 DLBCL cell lines known to be biologically dependent on BCL6 (OCI-Ly1, OCI-Ly7, and OCI-Ly10).^{11,14} Growth inhibition was measured by a metabolic viability assay and verified by trypan blue exclusion and was performed in biologic quintuplicates. The antilymphoma activity of BPI is dependent on the balance between cell penetration, stability, and binding to BCL6. Our goal was to identify peptides that potently and specifically inhibit BCL6 within lymphoma cells and that would be biologically active after a single dose. Figure 1 summarizes the data comparing successive generations of new peptides. For all peptides, the GI₅₀ is represented as the total amount of peptide administered over the course of the 48-hour treatment period (eg, for recombinant BPI, the GI₅₀ of 11.3 μM is a 48-hour total, so that an average of 900 ng peptide was administered at each 4-hour interval). To rule out nonspecific actions of these peptide derivatives, we used 2 types of negative controls. One set of control peptides contained an SI→AA mutation in the BBD, which we previously showed greatly impairs binding to the lateral groove and does not antagonize BCL6.¹¹ The other set of controls contained only the non-BBD portion of each peptide variant. Neither the mutant nor truncated peptide controls exhibited anti-BCL6 activity in DLBCL cells (Figure S1). Because both types of controls perform identically, in the remainder of the experiments only the truncated form was used for economic and ease-of-synthesis reasons. As an additional negative control, all peptides were also tested against the OCI-Ly4 DLBCL cell line, which we previously showed to be biologically independent of BCL6.^{11,14}

A synthetic peptide (peptide S1 in Figure 1) was next generated, containing only the TAT domain along with the 21 amino acids of the BBD motif. S1 proved to be difficult to synthesize for technical reasons pertaining to amino acid cleavage and was not active compared with the original BPI molecule. One possible reason for this could be charge interference between the negatively charged

Denomination	Peptide structure	GI ₅₀ (mean ± 95%CI)	Dose frequency
R	His6-TAT-Ha tag-GLVATVKEA-GRSIHEIPR-EEL	11.3 ± 3 μM	12
S1	TAT-GLVATVKEA-GRSIHEIPR-EEL	>100 μM	NA
S2	TAT-GRSHEIPRG	21.7 ± 3.2 μM	12
S3 L-BPI	Fu-TAT-GRSHEIPRG	14.2 ± 2 μM	12
S4	Fu-TAT-GRSHEIPRG	14.4 ± 2.2 μM	8
S5	GRPIEHISR-TAT-Fu	> 100 μM	NA
S6.1	GRGIEHISR-TAT-Fu	18 ± 3 μM	1
S6.2 RI-BPI	TAT-GRGIEHISR-Fu	16.5 ± 3.2 μM	1
S6.3	TAT-Fu-GRGIEHISR	25.3 ± 3.4 μM	1
S7	TAT-GRGIEHISR	96 ± 5 μM	1

Figure 1. Rational design of a BCL6 peptide inhibitor. The figure shows the structure, average GI₅₀, and dose frequency (ie, the number of doses given over a 48-hour period) for successive versions of BPI. GI₅₀ for the different peptides is an average of those obtained in the OCI-Ly1, OCI-Ly7, and OCI-Ly10 DLBCL cell lines. Each peptide and its respective control were tested at multiple doses and frequencies, with the goal of reaching the same potency as recombinant BPI with a single dose administration. The S3 and S6.2 (RI-BPI) peptides (shown in bold) were selected for further studies for the rest of the experiments shown in this article. GI₅₀ indicates growth inhibitory concentration 50%; DF, dose frequency during a 48-hour interval; R, recombinant; S, synthetic; NA, not applicable; light-gray background, L peptides; white background, L-D hybrid peptides; and dark-gray background, D peptides.

EEL tail of BPI and the positively charged TAT domain. To overcome this limitation, we generated shorter peptides that are easier to synthesize and lack the EEL motif. To select the most active BBD residues, we first analyzed the structure of the BCL6-SMRT interface. We noted that a sequence of 9 SMRT BBD amino acids (GRSHEIPR) make the greatest number of contacts to BCL6 and form a loop deep within the interface between BTB monomers.¹⁰ The TAT-GRSHEIPR peptide displayed an average GI₅₀ of 21.7 μM when administered at a dose frequency of 12 (ie, 1.8 μM per dose), suggesting that shorter BPI forms could retain the activity of the longer peptide and might be viable substrates for further derivation (peptide S2 in Figure 1).

Inclusion of a fusogenic motif enhances the activity of BPI

Combination with a TAT-fusogenic peptide can enhance release of cell-penetrating peptides from within macropinosomes.¹² Accordingly, we found that coadministration of the S2-BPI with a TAT-fusogenic peptide (Fu) could significantly enhance its antilymphoma activity in BCL6-dependent DLBCL cells but not in the BCL6-independent OCI-Ly4 cell line (Figure S1). Because administering 2 peptides is less efficient and more costly than giving a single peptide, we wondered whether including the fusogenic motif within S2 might offer an equivalent benefit. A mass-equivalent dose of the combined Fu-TAT-GRSHEIPR (S3) peptide was similar in efficacy to the concomitant administration of S2 plus fusogenic peptides, suggesting that the built-in capacity to enhance release of peptides from macropinosomes could improve the efficacy of BPI. The average GI₅₀ of S3 was 14.2 μM when administered every 4 hours (1.2 μM per dose).

RI-BPI is a stable drug-like BCL6 inhibitor

Synthesis of cell-penetrating peptides in the retroinverso configuration was shown to enhance their biologic activity because they retain a similar structural configuration but are resistant to cleavage by serum or cellular proteases.¹⁵ It was previously shown that retroinverso TAT and fusogenic motif are fully functional.¹⁵ To

determine whether peptide instability was solely the result of cleavage of the TAT, fusogenic motif, or the BBD, a hybrid form of BPI (S4) was generated containing retroinverso TAT and Fu with the normal L-amino acid GRSHEIPR motif (Figure 1). The S4-BPI displayed a GI₅₀ of 14.4 μM, identical to the all L version, even when administered at longer intervals (every 6 hours, dose frequency = 8). The data suggest that, although modifying TAT and Fu improves the stability of the peptide, loss of BBD function was still a limiting factor. However, when the entire peptide was built in retroinverso configuration (S5), it no longer displayed specific activity (Figure 1).

BPI is an unstructured peptide that adopts a pseudostructure when bound to BCL6.¹⁰ One possible explanation for loss of activity was the presence of a proline residue (P) within the GRSHEIPR motif because proline adopts a stereospecific conformation that would alter the shape of the peptide in the retroinverso configuration. Therefore, we tested whether switching from a proline to a glycine would restore the function of the BBD motif, presumably by allowing it sufficient flexibility to adopt its bound conformation. Three versions of the full retroinverso peptide with P to G mutations were generated, each containing the BBD in a different order in relation to TAT and Fu sequences. All 3 of these peptides (S6.1, S6.2, and S6.3 in Figure 1) displayed powerful antilymphoma activity against BCL6-dependent but not BCL6-independent DLBCLs cells, even when administered as a single dose (GI₅₀ of 18 μM, 16.5 μM, and 25.3 μM, respectively). Therefore, maximal biologic activity was achieved by converting the entire BPI molecule into a protease-resistant form.

Finally, we wondered whether the improved stability of retroinverso BPI might render it unnecessary to include a fusogenic motif and allow for a shorter peptide to be used (Figure 1). However, the retroinverso TAT-BBD (S7-BPI) was significantly weaker than the fusogenic-containing S6 peptides.

RI-BPI is a specific inhibitor of BCL6 transcriptional repressor function

We next wished to validate whether the most promising derivative peptide still retained the specific anti-BCL6 properties of the parent recombinant molecule. We chose the S6.2-BPI for all subsequent studies because it was the most potent version of RI-BPI and was also the easiest to generate on a peptide synthesizer (from here on, S6.2 is referred to as RI-BPI). To determine whether RI-BPI could still bind to BCL6, we performed coimmunoprecipitations between BCL6 and a biotinylated form of RI-BPI. BCL6 polyclonal antibody or an IgG control was used to capture BCL6 from lysates of OCI-Ly1 cells exposed to RI-BPI^{biotin} followed by sodium dodecyl sulfate-polyacrylamide gel electrophoresis and immunodetection using avidin-horseradish peroxidase (HRP) conjugates (Figure 2A). BCL6 readily captured RI-BPI, indicating that this peptide retained the ability to bind to its target. We previously showed that BPI specifically blocks the repressor activity of the BCL6 BTB domain but not that of other related transcriptional repressors.¹¹ Likewise, RI-BPI could specifically inhibit, in a dose-dependent fashion, the repressor activity of the BCL6 BTB domain but did not affect the repressor activity of the BTB domains from the Kaiso, HIC1, or PLZF proteins (Figure 2B). The mechanism of action of BPI consists of occupying the lateral groove of the BCL6 BTB domain, thus impeding recruitment of the SMRT and N-CoR corepressors to BCL6 target genes.¹¹ We performed chromatin immunoprecipitations in OCI-Ly1 cells exposed to RI-BPI and showed that the peptide was able to exclude SMRT and N-CoR from the BCL6 repression complex that forms

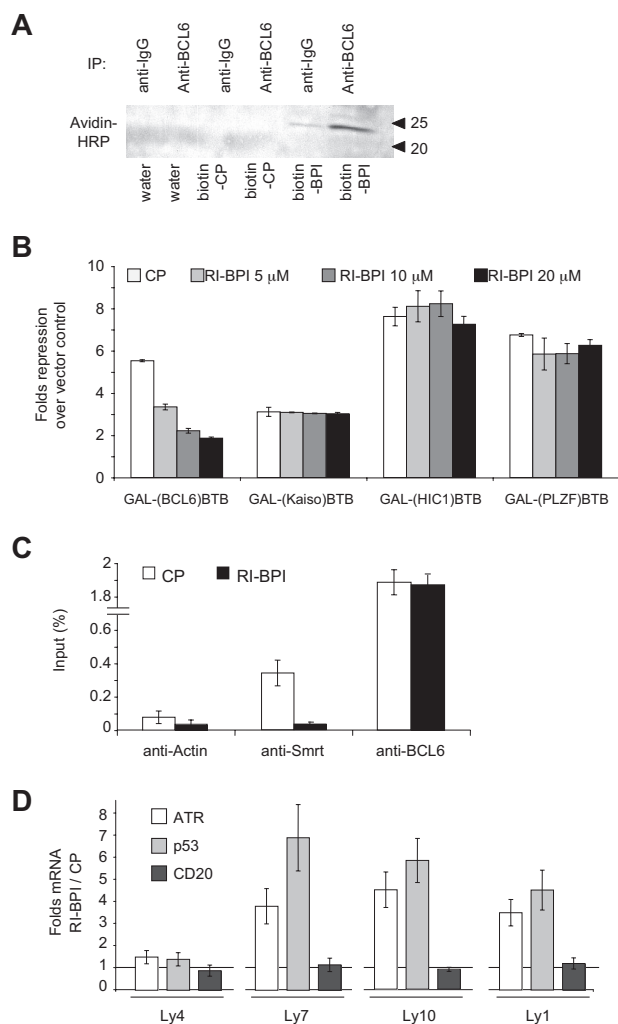


Figure 2. RI-BPI specifically inhibits the transcriptional and biologic function of BCL6. (A) BCL6 immunoprecipitation (IP) in OCI-Ly1 cell lysates after exposure to RI-BPI^{biotin} or CP^{biotin} (control) peptides. Anti-IgG was used as control for the IP. Detection of complexes was done using avidin-HRP conjugates. (B) Reporter assays performed in 293T cells transfected with BTB-fusion constructs as indicated. Cells were exposed to control peptide (□) or RI-BPI 5 μ M (▤), 10 μ M (▥), or 20 μ M (■). Fold repression is expressed versus the effect of each dose on a GAL4-DBD vector control for each experiment, relative to a TK-*Renilla* internal control. (C) Chromatin IP from OCI-Ly1 cells treated with CP 20 μ M (□) or RI-BPI 20 μ M (■) using antibodies against SMRT, BCL6, and actin (as a negative control) and amplifying the promoter region surrounding the BCL6 binding site on the *TP53* gene by quantitative PCR. Results are expressed as percentage relative to the input. (D) Real-time detection of mRNA of the endogenous BCL6 target genes *ATR* (□) and *TP53* (▤), and the control gene *CD20* (■), performed in the BCL6-dependent cell lines OCI-Ly7, OCI-Ly10, and OCI-Ly1 and in the BCL6-independent cell line OCI-Ly4, after treatment with RI-BPI 20 μ M and CP 20 μ M. Results are expressed as fold change in mRNA abundance mediated by RI-BPI over CP.

on the *TP53* promoter but did not affect the binding of BCL6 (Figure 2C). In accordance with these results, RI-BPI could reactivate the important BCL6 target genes *ATR* and *TP53* in BCL6-dependent DLBCL cells (OCI-Ly7, OCI-Ly10, and OCI-Ly1) but had no effect on OCI-Ly4 DLBCL cells (Figure 2D). BCL6 is required for formation of GCs in response to T cell-dependent antigens.^{1,2} We previously showed that recombinant BPI could attenuate formation of GCs when administered to immunized mice.¹¹ To determine whether RI-BPI could also block the activity of BCL6 in vivo, we administered 500 μ g RI-BPI or control peptide intraperitoneally after inducing a T-cell immune response in C57BL/6 mice ($n = 5$ per group). This dose was selected based on the GI₅₀ of DLBCL cells, which we previously showed are

similar in sensitivity to BPI as primary centroblasts.³ After 7 days of injections, the animals were killed and examined for formation of GCs. The architecture of lymphoid tissue and follicles was identical in RI-BPI and control peptide-treated animals, indicating that there was no general toxicity to the lymphoid organs. However, formation of GCs was significantly reduced in RI-BPI-exposed animals (Figure S2). Taken together, these data indicate that RI-BPI is a specific inhibitor of BCL6-mediated transcriptional repression that can inhibit the biologic effects of BCL6 in vivo.

RI-BPI selectively kills BCR-type DLBCL cells

A comprehensive unsupervised clustering analysis of a large cohort of DLBCL patients indicated the existence of 2 cell B-cell autonomous gene expression signatures.¹⁶ DLBCL cells featuring a B-cell receptor (BCR) activation signature expressed BCL6 and were selectively sensitive to BPI, whereas DLBCL cells with an oxidative phosphorylation (OxPhos) signature were resistant to BPI, regardless of whether they expressed BCL6.¹⁴ Accordingly, we found that the BCR-type DLBCL cell lines SU-DHL4, SU-DHL6, OCI-Ly1, OCI-Ly7, OCI-Ly10, OCI-Ly3, and Farage¹⁴ were all sensitive to RI-BPI, whereas the OxPhos cell lines Toledo, Karpas422, Pfeiffer, and OCI-Ly4 were resistant ($P < .001$, Figure 3). Like the original full-length form of BPI, RI-BPI retains specific activity against the BCL6-dependent BCR-type DLBCL cells.

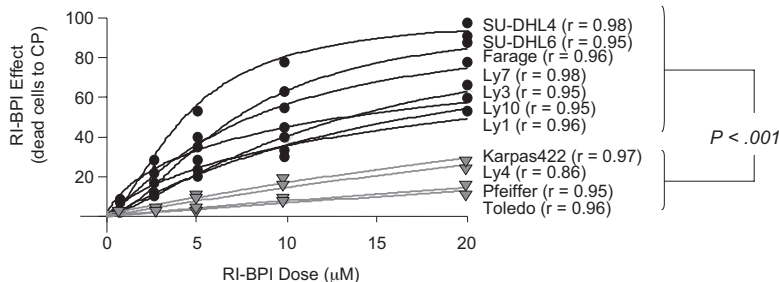
RI-BPI displays superior serum and tissue permanence

To test whether RI-BPI could perform as an antilymphoma therapeutic agent in vivo, we first wished to know whether it could penetrate tumor cells after parenteral administration through a distal site and whether it was more stable in vivo than L-amino acid BPI (L-BPI). For this purpose, 10⁷ SU-DHL4 cells were injected into the right flank of 12 SCID mice and allowed to form tumors. Once tumors reached approximately 1 g, animals were injected with a single dose of 500 μ g biotinylated RI-BPI or biotinylated S3 L-BPI and killed at 0, 0.25, 0.5, 1, 6, and 24 hours after peptide administration. An avidin-based enzyme-linked immunosorbent assay (ELISA) of serum peptide levels showed that both L-BPI and RI-BPI levels peaked 30 minutes after intraperitoneal injection (Figure 4A). However, the peak concentration of RI-BPI was double that of L-BPI (437 \pm 20 ng/mL vs 202 \pm 25 ng/mL, $P > .001$), possibly reflecting the fact that D-peptides are resistant to serum proteases. RI-BPI also reached a higher peak at the 0.25-hour time point. Histochemistry of tumors at the same time points showed that RI-BPI penetrated tumors more rapidly and persisted longer than L-BPI (Figure 4B). Peak concentrations in tissue of L-BPI occurred within 30 to 60 minutes, whereas in contrast RI-BPI was present at equivalent levels between 60 minutes and 6 hours and was still detectable in tumor cells 24 hours after administration (Figure 4B). Although this method of detection is indirect, taking into account the consistency in serum and tissues parameters, as well as the differences seen between L-BPI and RI-BPI, we have confidence that the biotin detected in tissues is peptide-bound biotin rather than free biotin. Therefore, RI-BPI reached higher serum levels and had a greater duration of tumor tissue residence, suggesting that RI-BPI would be a superior drug-like molecule for preclinical trials of antilymphoma targeted therapy.

RI-BPI effectively suppresses lymphoma growth in vivo

To evaluate the antilymphoma activity of BPI, a preclinical study was performed in which 2 BCR DLBCL cell lines (SU-DHL4 and SU-DHL6) were each injected into the right flank of 20 SCID mice

Figure 3. RI-BPI selectively kills BCR-type DLBCL cells. Dose-response curves for RI-BPI in a panel of 11 DLBCL cell lines. The x-axis shows the dose of BPI in micromoles. The y-axis shows the effect of RI-BPI compared with CP on cell viability. ● indicates BCL6-dependent cell lines (BCR-type); and ▼, BCL6-independent (OxPhos-type) cell lines. The goodness-of-fit for the experimental data to the median-effect equation is represented by the linear correlation coefficient (*r*) obtained from the logarithmic form of this equation. There was a statistically significant difference between the average of the GI₅₀ values of BCL6-dependent versus BCL6-independent cell lines (*P* < .001, *t* test).



and allowed to form tumors. Once palpable tumors were detected, pairs of mice were randomized to receive either 150 µg (*n* = 5) or 500 µg (*n* = 5) per day of RI-BPI or control peptide (*n* = 10). In addition, one OxPhos cell line (Toledo) was also implanted in SCID mice (*n* = 8) and treated with the 500-µg dose of RI-BPI or similar doses of control peptide as a negative control. Both the size and weight of tumors from RI-BPI treated animals were markedly reduced in a dose-dependent manner in both BCR cell lines, but not in the OxPhos tumors (Figures 5A,6A). The tumors in SU-DHL4 and SU-DHL6 mice were significantly smaller than their respective control at both dose levels (*P* = .001 and *P* = .002 for RI-BPI 150 µg, respectively, and *P* > .001 and *P* = .001 for RI-BPI 500 µg, respectively) (Figure 5A). The effect was dose-dependent because 500 µg RI-BPI more profoundly suppressed tumor growth than the 150-µg dose in both cell lines (SU-DHL4, *P* = .05; and SU-DHL6, *P* = .018) (Figure 5A). The tumor mass was also significantly reduced in a dose-dependent manner by RI-BPI (Figure 5B). At the moment of establishing the mouse xenotransplant models of human DLBCL, we found that the levels of human β2 microglobulin in mouse serum were closely correlated (*r* > 0.90) with tumor mass for all the cell lines tested, including SU-DHL4 (Figure S4), SU-DHL6, and Toledo cells. The levels of serum human β2 microglobulin by ELISA were significantly reduced by BPI in the xenograft experiments compared with their respective controls (Figure 5C). Using tumor growth to critical mass (10× from the initial mass) as a surrogate for survival, both the 150-µg (*n* = 10) and the 500-µg (*n* = 10) doses of RI-BPI increased the survival compared with control (*n* = 20) (Figure 5D, Kaplan-Meier survival curve, Gehan-Wilcoxon test *P* < .001 for

multiple samples and Cox F test, *P* = .001 and *P* = .05 for RI-BPI 150 µg vs control, and RI-BPI 150 µg vs RI-BPI 500 µg, respectively). There was no difference in tumor mass, tumor volume, and human β2 microglobulin in serum RI-BPI 500 µg and control-treated tumors for the Toledo cell xenografts (Figure 6).

Histologic examination of tumors revealed an increased fraction of cells undergoing apoptosis (by TdT-mediated dUTP nick end labeling (TUNEL) assay) in RI-BPI-treated animals (Figure 7A). There was no difference in apoptosis between RI-BPI and control-treated tumors for the Toledo cell xenografts (Figure 6D). The proliferative index measured as percent of cells staining for proliferating cell nuclear antigen by immunohistochemistry was also significantly decreased (Figure 7B). SU-DHL4 xenografts treated with control presented 29.6% plus or minus 6.4% nonproliferating cells compared with 75.2% plus or minus 3.12% and 78.2% plus or minus 2.2% of RI-BPI 150 µg (*P* < .001) and 500 µg (*P* < .001) treated mice, respectively. SU-DHL6 xenografts treated with control showed 40% plus or minus 3.5% nonproliferating cells compared with 66% plus or minus 2.3% and 65.6% plus or minus 4.8% of RI-BPI 150 µg (*P* < .001) and 500 µg (*P* < .001) treated mice, respectively. In concordance with these results, the mitotic index of RI-BPI-treated xenografts was also significantly reduced (Figure 7C). RI-BPI mediates its effects by overcoming BCL6-mediated transcriptional repression. To determine whether RI-BPI can induce expression of key BCL6 target genes in tumor xenografts, the mRNA abundance of p53 and ATR was measured by quantitative PCR. RI-BPI induced both genes in a dose-dependent manner in DLBCL xenografts (Figure 7D). Taken

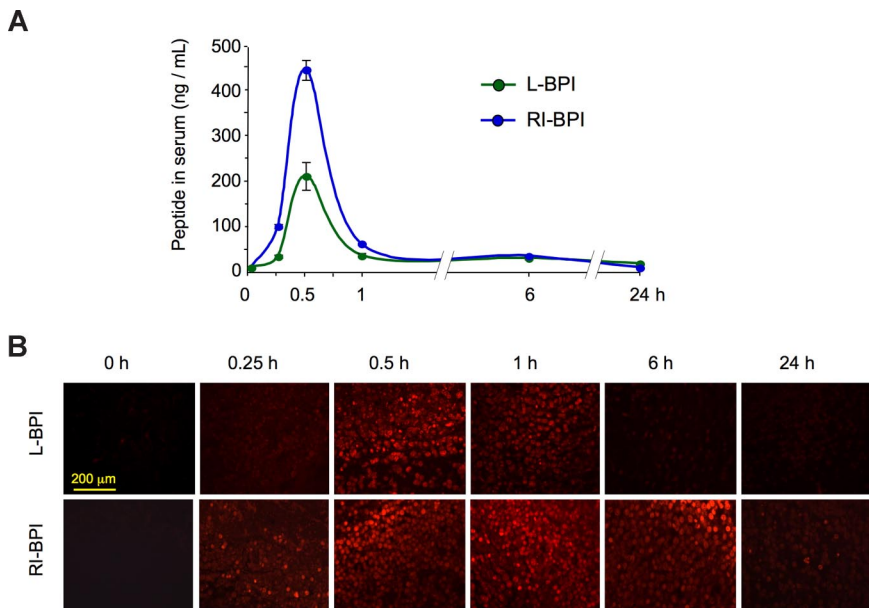


Figure 4. RI-BPI effectively distributes to lymphomas after parenteral administration. (A) The serum concentration of RI-BPI^{biotin} and L-BPI^{biotin} was determined after the intraperitoneal administration of 500 µg to mice carrying SU-DHL4 xenografts. Serum was taken at several time points (x-axis), and the concentration of biotinylated peptides was determined by chemical reaction with avidin-HRP (y-axis). (B) Histochemistry of the SU-DHL4 xenografts injected with RI-BPI^{biotin} and L-BPI^{biotin} performed at similar time points as in panel A. The presence of peptide was detected using Texas Red-avidin conjugates followed by fluorescence microscopy. Slides were mounted with permanent mounting medium (Vectashield Hard set; Vector Laboratories, Burlingame, CA) to prevent photobleaching. Slides were viewed with a fluorescent microscope (AxioSkop 2; Carl Zeiss, Jena, Germany) using a Plan-neofluar lens at a 10×/0.50 air objective and a 25×/0.80 oil objective. Images were acquired using a color camera (AxioCam; Carl Zeiss), and were processed using Axiovision software (Carl Zeiss).

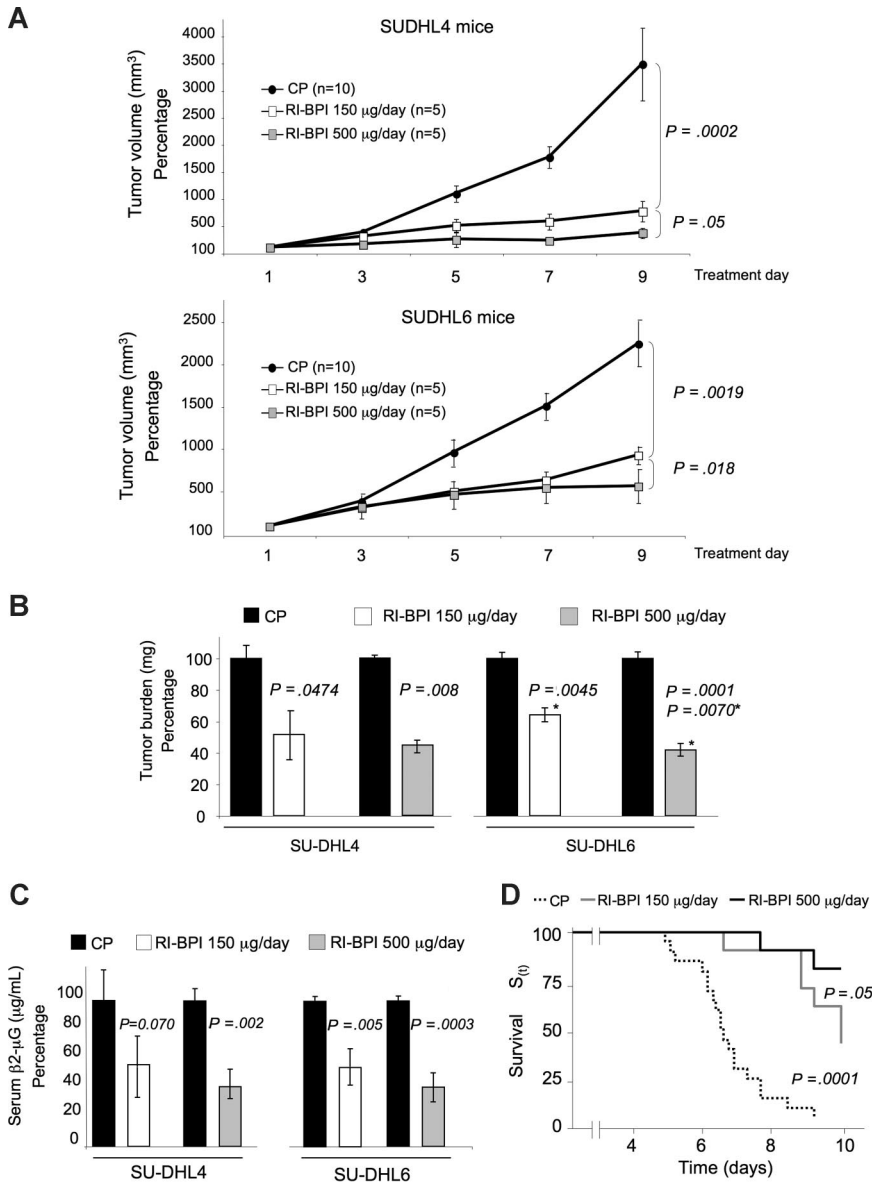


Figure 5. RI-BPI has antilymphoma activity in vivo.

(A) Tumor growth plots in SUDHL4 and SUDHL6 xenografted mice treated with control (●) or RI-BPI at 150 μg/day (□) or at 500 μg/day (■) for 10 consecutive days. The control peptide group includes mice treated with both the 150 and 500 μg/day doses, which were pooled to facilitate visualization. The y-axis represents the percentage of tumor volume (in mm³) compared to day 1 of treatment and x-axis represents treatment day. (B) Tumor burden (in milligrams) at day 10 in control (■), RI-BPI 150 μg/day (□), and RI-BPI 500 μg/day (■) treated SUDHL4 and SUDHL6 mice. (C) Serum levels of human β₂-microglobulin (measured in micrograms per milliliter and expressed as percentage to their respective controls) at day 10 in control (■), RI-BPI 150 μg/day (□), and RI-BPI 500 μg/day (■) treated SUDHL4 and SUDHL6 mice. (D) Kaplan-Meier survival curves for the pooled mice treated with control (dashed black line), 150 μg/day (gray line), and RI-BPI 500 μg/day (black line). A positive event was defined preanalysis as either death of the animal or tumor equal to 10 times the initial volume, whichever occurs first.

together, these data indicate that therapeutic targeting of BCL6 with RI-BPI is an effective antilymphoma strategy in vivo.

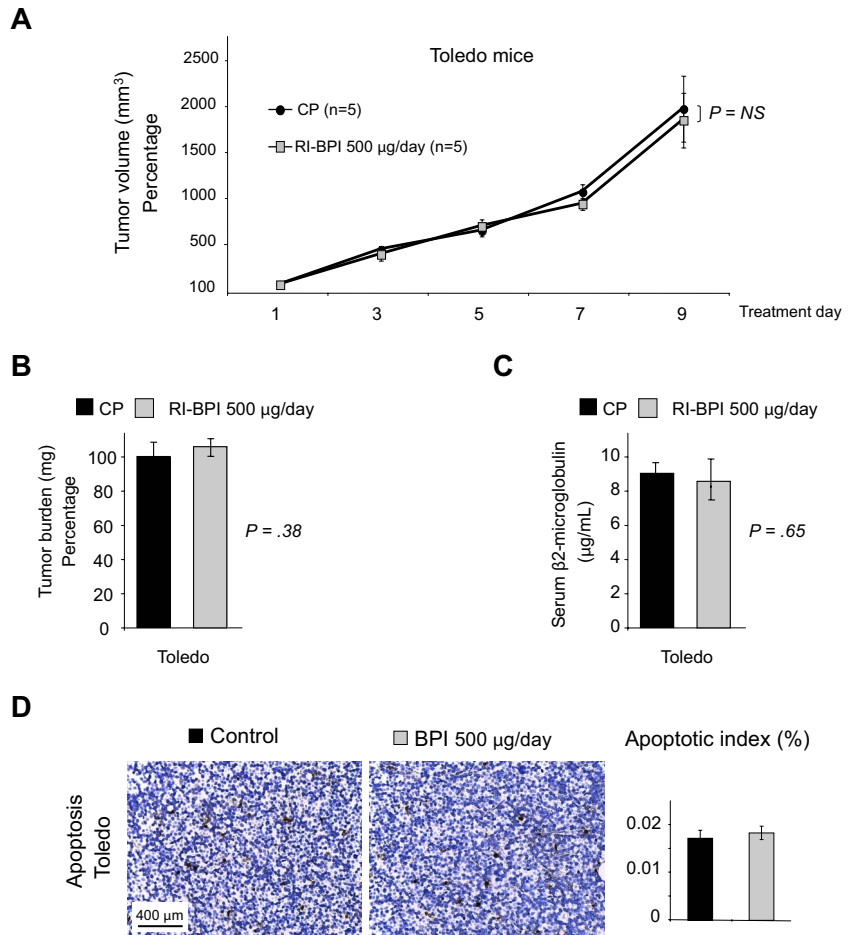
RI-BPI does not induce toxicity or immunogenicity

To determine whether RI-BPI could induce toxicity in vivo, a cohort of mice (n = 13) were exposed to intraperitoneal injections of 500 μg RI-BPI daily for 21 days (n = 5) or to 500 μg RI-BPI weekly for 52 weeks (n = 3). None of the animals exhibited signs of weight loss, failure to thrive, or illness, and none of the animals died. Histologic examination of tissues, including intestines, kidney, liver, lung, spleen, and myocardium, revealed normal architecture and cellular composition, comparable with normal controls (Figure S4). We wondered whether this apparent lack of toxicity could be the result of the development of antibodies against the peptides. Serum was collected from all mice treated at both the 21-day and 52-week time courses and examined by ELISA for antibodies immunoreactive to RI-BPI (data not shown). None of the mice developed antibodies able to bind to RI-BPI. Therefore, administration of RI-BPI in a mammalian model organism was safe and nonimmunogenic, even after prolonged exposure.

RI-BPI can specifically kill primary human DLBCL cells

Because RI-BPI is a candidate molecule for the treatment of human lymphomas, we wished to know whether primary DLBCLs could also respond to this drug. Single-cell suspensions were obtained from 29 diagnostic lymph node biopsy specimens and exposed to 10 μM RI-BPI or control peptide for 48 hours (Figure 8). For a majority of the cases, the diagnosis associated with the samples was blinded to the experimentalist. The impact of RI-BPI on viability of these specimens was determined by metabolic labeling in quadruplicate. Nine cases were diagnosed as nonmalignant reactive lymph nodes and were not affected by RI-BPI. Two cases each of T-cell lymphoma and Hodgkin disease were also insensitive to RI-BPI. A miscellaneous group (consisting of one head and neck squamous cell carcinoma, one marginal zone lymphoma, one chronic lymphocytic leukemia, and one thyroid carcinoma) were also unresponsive. Among the 12 DLBCLs, 11 cases were positive for BCL6 expression by immunohistochemistry. Nine of 11 BCL6-positive cases displayed greater than 25% loss of viability in response to RI-BPI. The one BCL6-negative DLBCL case was not

Figure 6. RI-BPI has no antilymphoma activity in the Toledo xenograft. (A) Tumor growth plot in Toledo (an OxPhos-type cell line) xenografted mice treated with control peptide (●) or RI-BPI 500 $\mu\text{g}/\text{day}$ (□) for 10 consecutive days. The y-axis represents the percentage of tumor volume (in mm^3) compared with day 1 of treatment, and the x-axis represents treatment day. (B) Tumor burden (in milligrams) at day 10 in control peptide (■) and RI-BPI 500 $\mu\text{g}/\text{day}$ (□) treated Toledo mice. (C) Serum levels of human $\beta 2$ -microglobulin (in micrograms per milliliter) at day 10 in control peptide (■) and RI-BPI 500 $\mu\text{g}/\text{day}$ (□) treated Toledo mice. (D) Representative images from Toledo mice tumors after being treated with control peptide (first column) or RI-BPI 500 $\mu\text{g}/\text{day}$ (second column), and assayed for apoptosis by TUNEL. The plot on the far right represents the apoptotic index (apoptotic cells over total cells) with the percentage of apoptotic cells in the y-axis for control peptide (■) and RI-BPI 500 $\mu\text{g}/\text{day}$ (□). Slides were mounted with permanent mounting medium (Vectamount; Vector Laboratories). Slides were viewed with a light microscope (AxioSkop 2; Carl Zeiss) using a Plan-neofluar lens at a $10\times/0.50$ air objective, a $25\times/0.80$ oil objective, a $40\times/0.90$ oil objective, and a $100\times/1.30$ oil objective. Images were acquired using a color camera (AxioCam; Carl Zeiss), processed using Axiovision software (Carl Zeiss), and scored using ImageJ software (National Institutes of Health, Bethesda, MD).



affected by RI-BPI. Therefore, most BCL6-positive human primary DLBCL samples were responsive to RI-BPI.

Discussion

As the most commonly involved oncogene in DLBCL, BCL6 is a potential therapeutic target. The facts that constitutive expression of BCL6 in animals causes DLBCL and that BCL6 loss of function can kill lymphoma cells support this notion.^{3,4,11,17,18} Like many transcriptional repressors, BCL6 mediates its actions indirectly, via protein-protein interactions with corepressor complexes that carry out the enzymatic activity of gene silencing. The BTB domain of BCL6 plays a critical role in this process by recruiting the SMRT and N-CoR corepressors to a lateral groove motif formed through homodimerization of BCL6 molecules.¹⁰ The amino acids that line the lateral groove of the BCL6 BTB homodimer make extensive contact with the BBD motif present in SMRT and N-CoR.¹⁰ These residues are unique to BCL6 and are not conserved on other members of the BTB-zinc finger family of transcription factors.¹⁰ The extensive nature of the interface between the BCL6 lateral groove and BBD motif may underlie the higher affinity for SMRT and N-CoR and greater repressor activity of BCL6 versus other BTB proteins^{10,19} and explain why BPI peptides do not inhibit other BTB domain-containing transcriptional repressors¹¹ (Figure 2).

A 120-amino acid recombinant peptide containing the SMRT BBD, a TAT peptide transduction domain, and other motifs for purification and immunodetection could specifically inhibit the

transcriptional repressor activity of BCL6 and kill DLBCL cells in vitro.¹¹ Although useful as a proof of principle, this form of BPI required frequent replenishment in tissue culture experiments and frequent administration in vivo to induce biologically significant BCL6 inhibition.¹¹ To generate a more drug-like BCL6 inhibitor comparable with other biologically targeted drugs, we modified the structure of BPI through a series of rationally designed steps. We first reduced the amount of BBD sequence to include only the 9 residues that make most extensive contact with the lateral groove. These residues form a macrocyclic structure that inserts deep within the lateral groove and makes multiple physical contacts with the 2 BTB monomers forming the walls of the groove.¹⁰ One barrier toward efficacy of TAT-delivered peptides is their tendency to become trapped within endosomes after macropinocytosis.¹³ To enhance endosomal release, we added a fusogenic motif derived from influenza virus, which can disrupt endosomal membranes as they become naturally acidified and thus facilitate release of peptides contained within into the cytoplasm. To decrease serum and tissue protease-dependent degradation, we converted BPI to a retroinverso configuration. Retroinverso peptides generated with D-amino acids are resistant to most proteases and can retain the proper secondary structural orientation needed for their activity. A single dose of retroinverso TAT-BBD-fusogenic form of BPI was equally potent as the original recombinant BPI given every 4 hours.

Although RI-BPI could bind BCL6 in vitro, the amplification of the signal that resulted from the biotin-streptavidin assay precluded us to accurately determine the K_d for this association. Nevertheless, we have

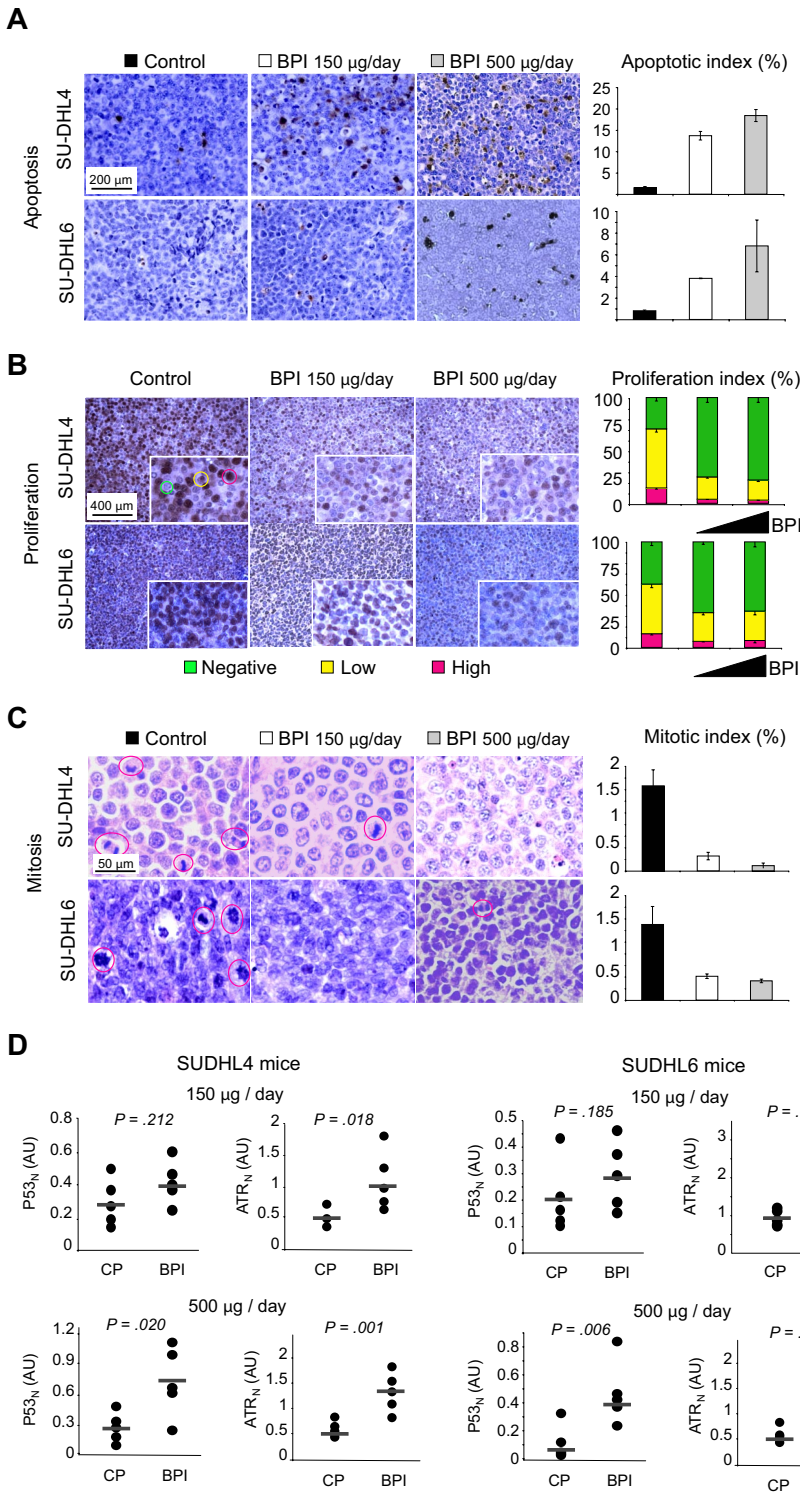


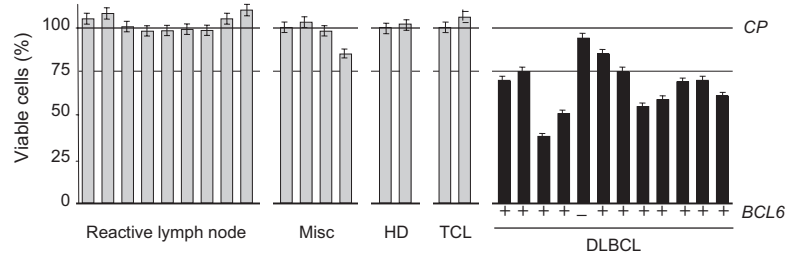
Figure 7. RI-BPI inhibits BCL6 transcriptional repression and induces DLBCL apoptosis in vivo. (A) Representative images from SU-DHL4 and SU-DHL6 mice tumors after being treated with control peptide (first column), RI-BPI 150 µg/day (second column), or RI-BPI 500 µg/day (third column), and assayed for apoptosis by TUNEL. The plot on the far right represents the apoptotic index (apoptotic cells over total cells) with the percentage of apoptotic cells in the y-axis for pooled control peptide doses (■), RI-BPI 150 µg/day (□), and RI-BPI 500 µg/day (▒) in the x-axis. (B) The same tumors as in panel A were assayed for proliferation by proliferating cell nuclear antigen immunostaining. Nuclei were classified as negative, low-intensity positive, and high-intensity positive as shown in the inset (digital zoom) of the SUDHL4 control tumor, by green, yellow, or red circles, respectively. The plot on the far right represents the proliferation index (using the same color coding for negative and positive cells) with the percentage of proliferating and nonproliferating cells in the y-axis for pooled control peptide samples (first stacking column), RI-BPI 150 µg/day (second stacking column), and RI-BPI 500 µg/day (third stacking column). (C) The same tumors were examined for the presence of mitotic cells. The plot on the far right represents the mitotic index (mitotic cells over total cells) with the percentage of mitotic cells in the y-axis in pooled control peptide samples (■), RI-BPI 150 µg/day (□), and RI-BPI 500 µg/day (▒). (A-C) Slides were mounted with permanent mounting medium (Vectamount; Vector Laboratories). Slides were viewed with a light microscope (AxioSkop 2; Carl Zeiss) using a Planneofluar lens at a 10×/0.50 air objective, a 25×/0.80 oil objective, a 40×/0.90 oil objective, and a 100×/1.30 oil objective. Images were acquired using a color camera (AxioCam; Carl Zeiss), processed using Axiovision software (Carl Zeiss), and scored using ImageJ software (National Institutes of Health, Bethesda, MD). (D) The mRNA abundance of *TP53* and *ATR* was determined in the same tumors by quantitative RT-PCR. The y-axis represents the normalized amount of mRNA in arbitrary units as measured by the relative standard curve method.

shown that RI-BPI is specific for BCL6, could disrupt endogenous BCL6 repression complexes, and reactivate critical target genes, such as the *ATR* and *TP53* cellular checkpoint mediators, in a similar order of magnitude as recombinant BPI. In a phenocopy of BCL6-deficient mice, RI-BPI inhibited the formation of GCs in the secondary lymphoid organs. Previous studies showed that BCL6 mediates survival of primary GC B cells and DLBCL cells in a SMRT- and N-CoR-dependent manner.^{3,11,20} Inhibition of the BCL6 lateral groove by BPI or RI-BPI does not affect these other BCL6 activities^{11,20,21} (data not shown). It seems probable that the severe inflammatory response

observed in BCL6-null mice, which is mostly the result of loss of BCL6 function in T cells,²² is also mediated through a different biochemical mechanism because this biologic effect was not observed in immunocompetent mice treated with RI-BPI for up to 1 year (Figure S5). Indeed, there was no evidence of toxicity in animals exposed to BPI for up to one year, raising the possibility that this form of targeted transcription therapy causing a partial rather than total loss of function of BCL6 could selectively inhibit the principal lymphomagenic effects of BCL6 without affecting many of its other biologic activities and thus avoiding potential side effects.

Figure 8. RI-BPI inhibits the growth of primary human DLBCLs.

Single-cell suspensions were obtained from lymph node biopsies of patients suspected of having DLBCL and were treated with either BPI 10 μ M (bars) or CP 10 μ M (line). □ indicates non-DLBCL samples; ■, DLBCLs. The y-axis represents the percentage of viable cells compared with control peptide, which is represented by the line at 100%. Error bars represent the SEM for triplicates. BCL6 status as assessed by immunohistochemistry is shown on the bottom for each DLBCL case. HD indicates Hodgkin disease; TCL, T-cell lymphoma; and Misc, miscellaneous diagnosis.



When DLBCL cells were implanted in mice, RI-BPI potently suppressed tumor formation in a dose-dependent manner. This was the result of both induction of cell death and growth arrest and was associated with induction of the important BCL6-regulated checkpoint genes *ATR* and *TP53*. Therefore, xenograft tumors formed from human BCR DLBCL cells remain biologically dependent on BCL6 and can be safely treated by BCL6-targeted therapy. Rational design of a peptidomimetic inhibitor of BCL6 demonstrates that this oncoprotein is an excellent therapeutic target for antilymphoma targeted therapy and has the potential to benefit patients with DLBCL.

A.M. was supported by the National Cancer Institute (Bethesda, MD; R01 CA104348), The Chemotherapy Foundation (New York, NY), The Sam Waxman Cancer Research Foundation (New York, NY), and the G&P Foundation (New York, NY) and is a Leukemia & Lymphoma Society (White Plains, NY) Scholar.

Acknowledgments

We thank Matty Scharff and Susan Buhl from the Albert Einstein College of Medicine (Bronx, NY) for their help in designing the anti-RI-BPI antibodies assay, as well as Gil Prive from the Ontario Cancer Institute (Toronto, ON) for helping with experimental design.

Authorship

Contribution: L.C.C. and A.M. designed the research, analyzed data, and wrote the paper; A.C. and S.F.D. designed the research and contributed vital new reagents and samples; and L.C.C., S.N.Y., K.H., J.M.P., and R.S. performed research and analyzed data.

Conflict-of-interest disclosure: The authors declare no competing financial interests.

Correspondence: Ari Melnick, Division of Hematology and Medical Oncology, Department of Medicine, Weill Cornell Medical College of Cornell University, 525 East 68th St, New York, NY 10065; e-mail: amm2014@med.cornell.edu.

References

- Ye BH, Cattoretti G, Shen Q, et al. The BCL-6 proto-oncogene controls germinal-centre formation and Th2-type inflammation. *Nat Genet*. 1997; 16:161-170.
- Dent AL, Shaffer AL, Yu X, Allman D, Staudt LM. Control of inflammation, cytokine expression, and germinal center formation by BCL-6. *Science*. 1997;276:589-592.
- Ranuncolo SM, Polo JM, Dierov J, et al. Bcl-6 mediates the germinal center B cell phenotype and lymphomagenesis through transcriptional repression of the DNA-damage sensor ATR. *Nat Immunol*. 2007;8:705-714.
- Phan RT, Dalla-Favera R. The BCL6 proto-oncogene suppresses p53 expression in germinal-centre B cells. *Nature*. 2004;432:635-639.
- Phan RT, Saito M, Basso K, Niu H, Dalla-Favera R. BCL6 interacts with the transcription factor Miz-1 to suppress the cyclin-dependent kinase inhibitor p21 and cell cycle arrest in germinal center B cells. *Nat Immunol*. 2005;6:1054-1060.
- Shaffer AL, Lin KI, Kuo TC, et al. Blimp-1 orchestrates plasma cell differentiation by extinguishing the mature B cell gene expression program. *Immunity*. 2002;17:51-62.
- Tunayaplin C, Shaffer AL, Angelin-Duclos CD, Yu X, Staudt LM, Calame KL. Direct repression of *prdm1* by Bcl-6 inhibits plasmacytic differentiation. *J Immunol*. 2004;173:1158-1165.
- Ye BH, Lista F, Lo Coco F, et al. Alterations of a zinc finger-encoding gene, BCL-6, in diffuse large-cell lymphoma. *Science*. 1993;262:747-750.
- Pasqualucci L, Neumeister P, Goossens T, et al. Hypermutation of multiple proto-oncogenes in B-cell diffuse large-cell lymphomas. *Nature*. 2001;412:341-346.
- Ahmad KF, Melnick A, Lax S, et al. Mechanism of SMRT corepressor recruitment by the BCL6 BTB domain. *Mol Cell*. 2003;12:1551-1564.
- Polo JM, Dell'Oso T, Ranuncolo SM, et al. Specific peptide interference reveals BCL6 transcriptional and oncogenic mechanisms in B-cell lymphoma cells. *Nat Med*. 2004;10:1329-1335.
- Wadia JS, Dowdy SF. Transmembrane delivery of protein and peptide drugs by TAT-mediated transduction in the treatment of cancer. *Adv Drug Deliv Rev*. 2005;57:579-596.
- Wadia JS, Stan RV, Dowdy SF. Transducible TAT-HA fusogenic peptide enhances escape of BCL6 target proteins after lipid raft macropinocytosis. *Nat Med*. 2004;10:310-315.
- Polo JM, Juszczynski P, Monti S, et al. Transcriptional signature with differential expression of BCL6 target genes accurately identifies BCL6-dependent diffuse large B cell lymphomas. *Proc Natl Acad Sci U S A*. 2007;104:3207-3212.
- Snyder EL, Meade BR, Saenz CC, Dowdy SF. Treatment of terminal peritoneal carcinomatosis by a transducible p53-activating peptide. *PLoS Biol*. 2004;2:E36.
- Monti S, Savage KJ, Kutok JL, et al. Molecular profiling of diffuse large B-cell lymphoma identifies robust subtypes including one characterized by host inflammatory response. *Blood*. 2005;105:1851-1861.
- Baron BW, Anastasi J, Montag A, et al. The human BCL6 transgene promotes the development of lymphomas in the mouse. *Proc Natl Acad Sci U S A*. 2004;101:14198-14203.
- Cattoretti G, Pasqualucci L, Ballon G, et al. De-regulated BCL6 expression recapitulates the pathogenesis of human diffuse large B cell lymphomas in mice. *Cancer Cell*. 2005;7:445-455.
- Melnick A, Carlile G, Ahmad KF, et al. Critical residues within the BTB domain of PLZF and Bcl-6 modulate interaction with corepressors. *Mol Cell Biol*. 2002;22:1804-1818.
- Parekh S, Polo JM, Shaknovich R, et al. BCL6 programs lymphoma cells for survival and differentiation through distinct biochemical mechanisms. *Blood*. 2007;110:2067-2074.
- Mendez L, Polo J, Yu J, et al. CtBP is an essential corepressor for BCL6 autoregulation. *Mol Cell Biol*. 2008; 28:2175-2186.
- Toney LM, Cattoretti G, Graf JA, et al. BCL-6 regulates chemokine gene transcription in macrophages. *Nat Immunol*. 2000;1:214-220.